arXiv:1309.4256v1 [astro-ph.GA] 17 Sep 2013

Evidence of non-thermal X-ray emission from HH 80

J. López-Santiago[1], C. S. Peri[2,3], R. Bonito[4,5], M. Miceli[5], J. F. Albacete-Colombo[6], P. Benaglia[2,3], E. de Castro[7]

ABSTRACT

Protostellar jets appear at all stages of star formation when the accretion process is still at work. Jets travel at velocities of hundreds of km s^{-1}, creating strong shocks when interacting with interstellar medium. Several cases of jets have been detected in X-rays, typically showing soft emission. For the first time, we report evidence of hard X-ray emission possibly related to non-thermal processes not explained by previous models of the post-shock emission predicted in the jet/ambient interaction scenario. HH 80 is located at the south head of the jet associated to the massive protostar IRAS 18162-2048. It shows soft and hard X-ray emission in regions that are spatially separated, with the soft X-ray emission region situated behind the region of hard X-ray emission. We propose a scenario for HH 80 where soft X-ray emission is associated to thermal processes from the interaction of the jet with denser ambient matter and the hard X-ray emission is produced by synchrotron radiation at the front shock.

Subject headings: Radiation mechanisms: non-thermal — X-rays: general — Herbig-Haro objects — ISM: jets and outflows — stars: pre-main sequence — stars: individual (IRAS 18162-2048)

1. Introduction

Knots observed in the optical band (Herbig-Haro objects, HH) originating from a YSO and traveling into the surrounding medium are associated to shock fronts and post-shock regions. The HH knotty structure along the jet axis, typically observed as a chain of knots, has been interpreted as pulses in the ejection of material by the star (see review in Bonito et al. 2010a), which can cause mutual interaction and collisions between knots (an example of collision between optical knots is discussed in Bonito et al. 2008, for an X-ray emitting jet). Hydrodynamic models predict X-ray emission by mechanical heating at the shock front, caused by the interaction between the jet and the ambient, with the shocked material reaching temperatures of 1 MK (Bonito et al. 2004), thus emitting in the soft X-rays.

Supersonic shock fronts and post-shock regions along the jet have been detected in a wide wavelength range, from radio to optical bands (Reipurth & Bally 2001, and references therein) and can be detected also in the ultraviolet (Ortolani & Dodorico 1980; Hollis et al. 1991; Liseau et al. 1996; Gómez de Castro & Verdugo 2001; Gómez de Castro & von Rekowski 2011; Coffey et al. 2012; Schneider et al. 2013). In recent years, several protostellar jets have been revealed also in X-rays (Pravdo et al. 2001, 2004; Favata et al. 2002, 2006; Bally et al. 2003; Kastner et al. 2005; Grosso et al. 2006; Güdel et al. 2008; Bonito et al. 2010a,b, 2011).

[1]Instituto de Matemática Interdisciplinar, S. D. Astronomía y Geodesia, Facultad de Ciencias Matemáticas, Universidad Complutense de Madrid, E-28040 Madrid, Spain

[2]Instituto Argentino de Radioastronomía (IAR), CCT La Plata (CONICET), C.C.5, 1894 Villa Elisa, Buenos Aires, Argentina

[3]Facultad de Ciencias Astronómicas y Geofísicas, Universidad Nacional de La Plata, Paseo del Bosque s/n, 1900 La Plata, Argentina

[4]Dipartimento di Fisica e Chimica, Università di Palermo, Piazza del Parlamento 1, 90134 Palermo, Italy

[5]INAF-Osservatorio Astronomico di Palermo, Piazza del Parlamento 1, I-90134 Palermo, Italy

[6]Universidad Nacional del COMAHUE, Monseñor Esandi y Ayacucho, 8500 Viedma, Río Negro, Argentina

[7]Dpto. de Astrofísica y CC. de la Atmósfera, Universidad Complutense de Madrid, E-28040 Madrid, Spain

The Herbig-Haro complex HH 80-81 was detected in X-rays by Pravdo et al. (2004). HH 80-81 is the south part of an extended jet whose main source is the high-mass protostar IRAS 18162-2048 ($L = 17000\,L_{\odot}$; Carrasco-González et al. 2010), which is situated at a distance of 1.7 kpc (Rodríguez & Reipurth 1989) in the direction of the Sagittarius arm. With a projected extension of $\simeq 5$ pc, this is one of the largest protostellar jets ever detected (see also Tsujimoto et al. 2004; Rodríguez et al. 2005; Carrasco-González et al. 2010). Pravdo et al. (2004) distinguished two X-ray sources coincident with HH 80: a soft X-ray source ($T \sim 1.5$ MK) related to HH 80A (the northern and brighter part of HH 80), and a hard source to the south of another H_{α} condensation (HH 80E) that they fitted with similar accuracy to both a high-temperature thermal model and a power-law with index ~ 1 (for a complete list of optical knots see Heathcote et al. 1998). From the analysis of *Chandra* spectra, the authors suggested that the hard X-ray source may be an embedded protostar, while the soft source is a region of shocked material associated to the jet.

The HH 80-81 complex has been extensively studied at radio frequencies. Martí et al. (1993) reported intensities and spectral indices for a number of radio bands using VLA observations. The authors indicated that radio emission from HH 80 and HH 81 is consistent with non-thermal radiation from relativistic electrons, according to measured spectral indices. More recently, Carrasco-González et al. (2010) showed that this jet is magnetized and linearly polarized. The latter is an indication of synchrotron radiation. The strength of the magnetic field at the base of the jet determined from the analysis of Carrasco-González et al. (2010) is $B \approx 0.2$ mG. Although there is no measurement of the field strength at the position of HH 80 and HH 81, models of precessing jets for IRAS 18162-2048 reproduce well the position of these two knots and those detected to the North (Masqué et al. 2012). This result has been interpreted as a proof of the resemblance between the ejection mechanism in both high– and low–mass stars.

Based on the most recent results from radio wavelengths and our analysis of the X-ray properties of HH 80 detected with both XMM and Chandra (see Section 2), we propose a new scenario for HH 80 in which the soft X-ray emission is produced in a shock front caused by the interaction of the jet with the ambient medium, while the hard X-ray emission is produced by synchrotron emission of electrons in the jet magnetic field. In the following sections we show a multiwavelength analysis of HH 80 that supports our hypothesis.

2. X-ray data analysis

2.1. *XMM-Newton* observation

We analyzed the *XMM-Newton* EPIC archive observation ID 0149610401 (obs. date: 2003-09-14) performed with the Medium filter by using the Full Frame Mode for the MOS (Turner et al. 2001) and pn (Strüder et al. 2001) cameras. The observation was pointed towards the central source IRAS 18162-2048. With a telescope's field-of-view of $30'$, this observation covers the whole jet, from HH 80N at the northeast to HH 80 and HH 81 at the southwest. We processed the data by using the Science Analysis System (SAS V12). Light curves, images, and spectra, were created by selecting events with PATTERN$\leq$12 for the MOS cameras, PATTERN$\leq$4 for the pn camera, and FLAG=0 for both. To reduce the contamination by soft proton flares, the event files were screened by adopting the sigma-clipping algorithm. The screened exposure times are 29 ks, 30 ks, and 23 ks for MOS1, MOS2, and pn, respectively. Fig. 1 shows the EPIC image of the source in the $0.5-1$ keV band. The image has been obtained by superimposing (with the $EMOSAIC$ task) the MOS1, MOS2, and pn images, taking account of the differences between MOS and pn effective areas, and is background-subtracted, vignetting-corrected, and adaptively smoothed (with the task $ASMOOTH$).

We performed the spectral analysis in the energy band $0.3-8$ keV using XSPEC V12.8. Spectra were extracted from the region shown in Fig. 1 and rebinned to achieve a signal-to-noise ratio per bin > 4. Spectral fittings were performed simultaneously on both MOS spectra and on the pn spectrum. The reported errors are at 90% confidence. We verified that an isothermal model of optically thin plasma (APEC model in XPSEC) cannot describe the observed spectra ($\chi^2 = 260$ with 33 degrees of freedom, hereafter dof) and significantly underestimates the high-energy part of

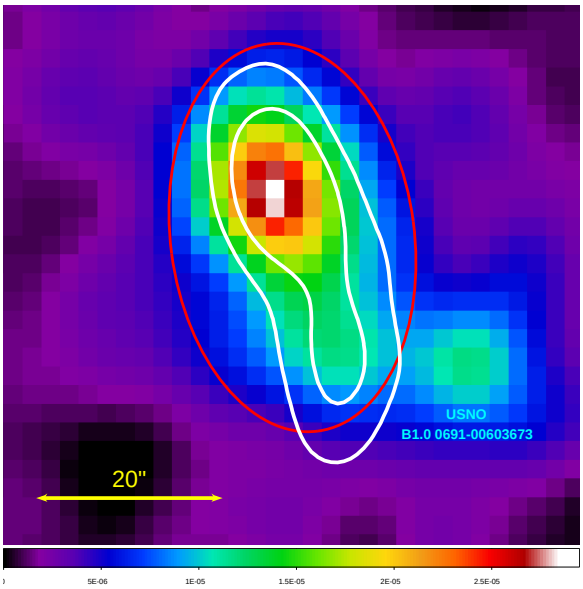


Fig. 1.— Count-rate image (MOS-equivalent counts per second per bin in the $0.3-1$ keV energy band). The bin size is $2''$, and the image is adaptively smoothed to a signal-to-noise ratio of ten. The region selected for the spectral analysis is shown in red. Radio contours from the data presented in Martí et al. (1993) are overplotted in white. North is up and East is to the left.

the spectrum showing systematic residuals above ~ 1 keV. We obtained a very good fit to the data ($\chi^2 = 29.1$ with 31 dof) by adding to the thermal model a power-law component. Figure 2 shows the pn spectrum[1] with the best fit model and residuals. The thermal component, with temperature $kT_1 = 0.11 \pm 0.03$ keV well describes the low energy part of the spectrum, while contribution of the power-law component, which shows a very flat spectral index $\Gamma = 0.8^{+0.3}_{-0.2}$, dominates above ~ 1.5 keV. We also adopted a model with two APEC components to investigate a possible thermal origin for the hard X-ray emission. Though this model provides an acceptable fit to the spectra ($\chi^2 = 33.7$ with 31 dof), it provides an unrealistically high value for the temperature of the hot plasma, $kT_2 > 27$ keV. Therefore, we conclude that the hard X-ray emission does not have a thermal origin.

[1]Only the pn spectrum is shown for clarity.

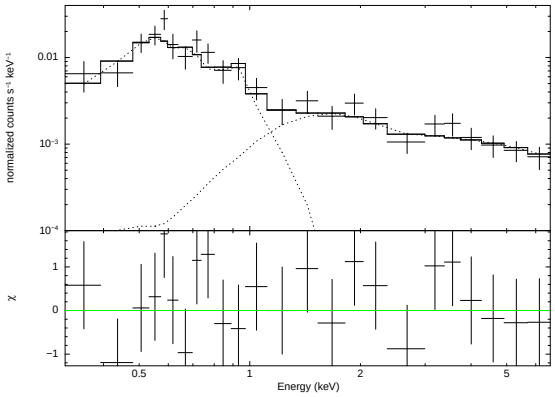


Fig. 2.— PN spectrum of HH80 (extracted from the region shown in Fig. 1) with the corresponding APECT+Power-law best-fit model and residuals. The contribution of each component is shown.

2.2. *Chandra* observation

HH 80 was observed twice with the Advanced CCD Imaging Spectrometer (ACIS) onboard the *Chandra* X-ray observatory (Obs. Ids. 2535 and 6405). HH 80 is off-axis in the latter and so, those data were not used for our study. During the observation performed in 2002, data were acquired in faint mode for a total of 37.7 ks.

Data reduction, starting with the level 1 event list provided by the pipeline processing tool of *Chandra*, was carried out with CIAO 4.4 and the CALDB 4.5.3 set of calibration files. We produced a level 2 event file using the *chandra_repro* CIAO task, taking advantage of the F-mode enhanced background, filtering and retaining only events with $grades = 0, 2, 3, 4, 6$ and $status = 0$. Since the images of the ACIS-S4 chip show a variable pattern of linear streaks, we created a new bad-pixel file to improve the streak detection efficiency in S4 chip. We filtered events in the 0.5-8 keV range. By performing a simultaneous spectral fitting of the Chandra dataset with the XMM dataset, we derived compatible results as described in Section 2.1.

Chandra/ACIS resolution allowed us to distinguish the soft and hard X-ray emitting components (see Fig. 3). In order to analyze the morphology of these two components of the HH 80 complex structure, we also applied the subpixel repositioning algorithm available in CIAO (EDSER) to the Chandra images to refine the

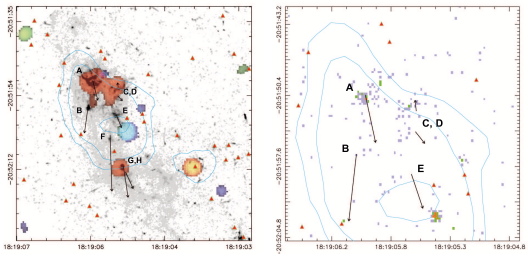


Fig. 3.— **Left:** WPC2 H_α image of HH 80 with *XMM-Newton* EPIC-pn contours and *Chandra* smoothed image overplotted in false color: red for 0.3–1.2 keV, green for 1.2–2.5 keV and blue for 2.5–4.5 keV. Coordinates are J2000. Proper motions are from Heathcote et al. (1998), transformed to J2000. Filled triangles are *Spitzer* sources in the [3.6] μm band of IRAC with $S/N \geq 2$. **Right: central region of HH 80. This is a refined *Chandra* image resulting from the sub-pixel repositioning algorithm.** The binning is 0.5. Contours, proper motions, triangles and flags are the same than in the left panel.

event positions (Li et al. 2004). The improved image can therefore be resampled at one-half of the native ACIS pixel scale ($0.5/2''$). Both the soft and the hard components show a hint of elongation which appears, if any, aligned with the jet axis and the proper motion of the E knot (see Fig. 3, right panel). Note that recently, an asymmetry in the Chandra point spread function (PSF) has been discovered located at position angle P.A. = 195 - roll angle $\pm$25 deg, corresponding to P.A. = 285.844 deg which is not coincident with the direction of the extension of the X-ray sources nor the jet axis.

3. Search for optical and infrared counterparts

We looked for counterparts to the different X-ray sources associated to HH 80 at other wavelengths, with the aim of discarding an extragalactic origin for the X-ray emission in this region. We analyzed data from the *Spitzer* mission and inspected the H_α image taken with the WFPC2 onboard the *Hubble* Space Telescope (Heathcote et al. 1998). From Fig. 3, it seems clear that there is no point-like source associated to the hard X-ray source (below knot E), while the soft X-ray sources are related to different H_α knots of the jet (precisely knots A-D).

The *Spitzer* Heritage Archive at the NASA, IPAC Infrared Science Archive contains one observation from the GLIMPSE project covering the region of HH 80-81 (AORKEY 21289984) and a pointed observation in map mode with both the IRAC, Infrared Array Camera (AORKEY 11069952) and the MIPS, Multiband Imaging Photometry for SIRTF (AORKEY 11072256). With a configuration with frame time 10.4 s, the pointed observation of HH 80-81 is substantially deeper, reaching limiting magnitudes in the [3.6] μm band $\simeq$ 20 mag for sources detected above $S/N = 2$ ($F \simeq 30$ μJy). We followed the procedure described in López-García et al. (2013) to find sources in this *Spitzer* observation and performed aperture photometry. Both panels in Fig. 3 show the infrared sources detected by us in the proximities of HH 80 (filled triangles). The only infrared source close to the hard X-ray source is located $> 5''$ to the North of the *Chandra* source and it is detected only in the [3.6] μm band with $S/N \simeq 2$. Given this low IR-signal and the size of the angular offset, any physical association is unlikely.

4. Discussion

HH 80-81 is the head of a jet whose origin is the massive protostar IRAS 18162-2048. The jet emits at radio frequencies (Martí et al. 1993) and this emission is linearly polarized (Carrasco-González et al. 2010). The region of HH 80 shows radio emission with negative spectral index $\alpha = -0.3$ (Martí et al. 1993), indicating that it is dominated by non-thermal radiation (e.g. Ginzburg & Syrovatskii 1964). In addition to HH 80-81, only a few young stellar objects show evidence of non-thermal radio emission in their outflows: Serpens triple radio source, Cepheus A East sources 1-7, W3(H_2O), L778 VLA 5 and IRAS 16547-4247 (see Carrasco-González et al. 2010, and references therein). Radio-synchrotron polarized emission has been detected only in IRAS 18162-2048.

The HH 80 *XMM-Newton* spectrum shows a soft component, which is compatible with thermal plasma emission at a temperature $\sim 10^6$ K, plus a hard component with a power-law spectrum

with index $\alpha \simeq 0.8$. *Chandra* is able to separate both spectral components spatially. The soft component is correlated with the denser H_α region (HH 80A, C and D). The hard component is located just in front of HH 80E in a region with low gas density (see Fig. 3).

Bonito et al. (2010b) results suggest that HH80/81 and probably also the X-ray emitting jet discovered by Tsujimoto et al. (2004) (TKH8), for which high velocities are needed to explain their spectra, are not compatible with the other soft X-ray emitting jets well modeled by the post-shock emission due to the jet/ambient interaction (as in the wide exploration of the parameter space performed also in Bonito et al. 2007). In Fig. 7 of Bonito et al. (2010b), in fact, both HH 80 and TKH8 cannot be described by the model of the emission from the post-shock formed by the jet/ambient interaction as in the cases of the other jets emitting soft X-rays; furthermore, the shock velocity deduced in these two jets is high with respect to the other soft jets.

The analysis of the morphology of the *Chandra*/ACIS detected source at sub-pixel resolution shows a hint of elongation of the hard component along the jet axis and the proper motion of the E knot (note that the PSF asymmetry has been computed and is not aligned with the jet axis but, on the contrary, it is almost perpendicular to the proper motion of the knots within the jet). Available Chandra/ACIS data allowed us to discriminate the two X-ray emitting components detected in HH 80: the soft component is almost coincident with the A knot, and the hard component is located along the jet axis further away with respect to the E knot and along its proper motion (see Fig. 3, right panel). A deeper Chandra observation could help in distinguishing the hard component morphology and in performing a spatially resolved spectral analysis of the different sources. Also with a time baseline of more than ten years, it will be possible to measure the proper motion of the source, if any, and compare with radio proper motions.

The hard X-ray source has been previously proposed to be an embedded protostar not related to the jet itself (see Pravdo et al. 2004). To explore this scenario, we looked for counterparts to the hard X-ray source in any photometric band, from optical to infrared. As we mentioned in Section 3, no counterpart was found down to 20 mag in the *Spitzer*/IRAC bands, neither in MIPS data. This result likely discards the scenario of the embedded protostar.

The possible relation of the hard X-ray source with a highly obscured AGN appears also unlikely. With a measured (unabsorbed) X-ray flux in the [0.3-10] keV energy band of $f_{\rm X} \sim 10^{-14}$ erg cm^{-2} s^{-1}, the source is quite bright in X-rays. According to the $\log N$-$\log S$ distribution of bright AGN (e.g. Della Ceca et al. 2004), the density of these objects at this flux is ~ 100 deg^{-2}. Following Combi et al. (2011), the probability that an AGN were detected inside the *XMM-Newton* contours is $P \sim 0.15$ (15%) and the probability that it were situated at less than $5''$ of the hard X-ray source is $P < 0.02$ (2%).

At a distance of 1.7 kpc, the X-ray luminosity of the hard X-ray source is $L_{\rm X} \simeq 3 \times 10^{30}$ erg s^{-1} ($f_{\rm X} \sim 10^{-14}$ erg cm^{-2} s^{-1} for the hard X-ray source). This is very close to the value expected by Bosch-Ramon et al. (2010) for secondary electrons and positrons from proton-proton collisions (see their Fig. 5 and Araudo & Rodríguez 2012). Note that the authors considered a particle density $n_c \sim 10^2 - 10^3$ cm^{-3}, bolometric luminosity $L_\star \simeq 2 \times 10^4$ L$_\odot$ and jet velocity at the base $v_j \sim 10^3$ km s^{-1} (see Table 1 of Bosch-Ramon et al. 2010, for a complete list of observed and derived parameters for HH 80). The magnetic field determined by the authors at the position of HH 80 is $B \sim 0.02$ mG. This is one order of magnitude lower than the magnetic field strength determined by Carrasco-González et al. (2010) at the base of the jet but consistent with the value expected at the distance of HH 80 from the star (Bosch-Ramon et al. 2010).

5. Conclusions

Supported by the results of our analysis of X-ray *Chandra* and *XMM-Newton* data and cross-correlation with optical and infrared databases, we propose a new scenario for the nature of the hard X-ray emission detected at the edge of HH 80. While the soft X-ray emission is produced in the post-shock region after interaction of the jet with dense medium, the hard X-ray emission is produced by synchrotron radiation of accelerated particles at the front-shock. The spectral index of the

power-law spectrum in both X-ray and radio wavelengths is consistent with this hypothesis. In addition, the X-ray luminosity assuming a distance of 1.7 kpc agrees well with the predictions by models of non-thermal emission for HH 80. This is the first evidence of non-thermal emission detected in X-rays for a stellar jet.

This work was supported by the Spanish Government (AYA2011-29754-C03-01 and AYA2011-29754-C03-03). C. S. P. was granted by the COSPAR Capacity Building Workshop Fellowship Program and the Universidad Nacional de La Plata to develop this work at the Universidad Complutense de Madrid. M. M. is supported through the ASI-INAF contract I/009/10/0. JFAC is a staff researcher of the CONICET and acknowledges support by grant PIP 2011 0100285. J. L.-S. would like to thank Drs. F. J. Carrera, P. G. Pérez-González and S. Mateos for fruitful discussion on spectral X-ray emission properties of AGN. We also acknowledges the referee of this manuscript for his/her suggestions and comments.

Facilities: XMM-Newton (EPIC). Chandra (ACIS). Spitzer (IRAC, MIPS).

REFERENCES

Araudo, A. T., & Rodríguez, L. F. 2012, American Institute of Physics Conference Series, 1505, 281

Bally, J., Feigelson, E., & Reipurth, B. 2003, ApJ, 584, 843

Bonito, R., Orlando, S., Peres, G., Favata, F., & Rosner, R. 2004, A&A, 424, L1

Bonito, R., Orlando, S., Peres, G., Favata, F., & Rosner, R. 2007, A&A, 462, 645

Bonito, R., Fridlund, C. V. M., Favata, F., et al. 2008, A&A, 484, 389

Bonito, R., Orlando, S., Peres, G., et al. 2010a, A&A, 511, A42

Bonito, R., Orlando, S., Miceli, M., et al. 2010b, A&A, 517, A68

Bonito, R., Orlando, S., Miceli, M., et al. 2011, ApJ, 737, 54

Bosch-Ramon, V., Romero, G. E., Araudo, A. T., & Paredes, J. M. 2010, A&A, 511, A8

Carrasco-González, C., Rodríguez, L. F., Anglada, G., et al. 2010, Science, 330, 1209

Coffey, D., Rigliaco, E., Bacciotti, F., Ray, T. P., & Eislöffel, J. 2012, ApJ, 749, 139

Combi, J. A., Albacete Colombo, J. F., Pellizza, L., et al. 2011, Ap&SS, 331, 53

Della Ceca, R., Maccacaro, T., Caccianiga, A., et al. 2004, A&A, 428, 383

Favata, F., Fridlund, C. V. M., Micela, G., Sciortino, S., & Kaas, A. A. 2002, A&A, 386, 204

Favata, F., Bonito, R., Micela, G., et al. 2006, A&A, 450, L17

Ginzburg, V. L., & Syrovatskii, S. I. 1964, The Origin of Cosmic Rays, New York: Macmillan

Gómez de Castro, A. I., & Verdugo, E. 2001, ApJ, 548, 976

Gómez de Castro, A. I., & von Rekowski, B. 2011, MNRAS, 411, 849

Grosso, N., Feigelson, E. D., Getman, K. V., et al. 2006, A&A, 448, L29

Güdel, M., Skinner, S. L., Audard, M., Briggs, K. R., & Cabrit, S. 2008, A&A, 478, 797

Heathcote, S., Reipurth, B., & Raga, A. C. 1998, AJ, 116, 1940

Hollis, J. M., Oliversen, R. J., Michalitsianos, A. G., Kafatos, M., & Wagner, R. M. 1991, ApJ, 377, 227

Kastner, J. H., Franz, G., Grosso, N., et al. 2005, ApJS, 160, 511

Li, J., Kastner, J. H., Prigozhin, G. Y., et al. 2004, ApJ, 610, 1204

Liseau, R., Huldtgren, M., Fridlund, C. V. M., & Cameron, M. 1996, A&A, 306, 255

López-García, M. A., López-Santiago, J., Albacete-Colombo, J. F., Pérez-González, P. G., & de Castro, E. 2013, MNRAS, 429, 775

Martí, J., Rodríguez, L. F., & Reipurth, B. 1993, ApJ, 416, 208

Masqué, J. M., Girart, J. M., Estalella, R., Rodríguez, L. F., & Beltrán, M. T. 2012, ApJ, 758, L10

Ortolani, S., & Dodorico, S. 1980, A&A, 83, L8

Pravdo, S. H., Feigelson, E. D., Garmire, G., et al. 2001, Nature, 413, 708

Pravdo, S. H., Tsuboi, Y., & Maeda, Y. 2004, ApJ, 605, 259

Reipurth, B., & Bally, J. 2001, ARA&A, 39, 403

Rodríguez, L. F., & Reipurth, B. 1989, Rev. Mexicana Astron. Astrofis., 17, 59

Rodríguez, L. F., Garay, G., Brooks, K. J., & Mardones, D. 2005, ApJ, 626, 953

Schneider, P. C., Eislöffel, J., Güdel, M., et al. 2013, A&A, 550, L1

Strüder, L., Briel, U., Dennerl, K., et al. 2001, A&A, 365, L18

Tsujimoto, M., Koyama, K., Kobayashi, N., et al. 2004, PASJ, 56, 341

Turner, M. J. L., Abbey, A., Arnaud, M., et al. 2001, A&A, 365, L27

This 2-column preprint was prepared with the AAS LaTeX macros v5.2.